Non-scanning Radiometer Results for Earth Radiation Budget Investigations

by

G. Louis Smith, Richard N. Green, Robert B. Lee, III and T. Dale Bess

Atmospheric Sciences Division

Langley Research Center

Hampton, Virginia 23681-001

and

David Rutan

Lockheed Engineering and Sciences Co.

144 Research Road

Hampton, Virginia 23666

Presented at

Eighth Symposium on Meteorological Observations and Instrumentation

Anaheim, California

January 17-22, 1992

Non-Scanning Radiometer Results for Earth Radiation Budget Investigations

by

G. Louis Smith[1], Richard N. Green[1], Robert B. Lee III[1], T. Dale Bess[1], and David Rutan[2]

1. Atmospheric Sciences Division, NASA, Langley Research Center, Hampton, VA 23681-0001
2. Lockheed Engineering and Sciences Co., 144 Research Road, Hampton, VA 23666

1. Introduction

The Earth Radiation Budget Experiment (ERBE) included non-scanning radiometers (Luther, 1986) flown aboard a dedicated mission of Earth Radiation Budget Satellite, and the NOAA-9 and -10 operational meteorological spacecraft (Barkstrom and Smith, 1986). The radiometers first began providing Earth radiation budget data in November 1984 and have remained operational, providing a record of nearly 8 years of data to date for researchers. Although they do not produce measurements with the resolution given by the scanning radiometers, the results from the non-scanning radiometers are extremely useful for climate research involving long-term radiation data sets. This paper discusses the non-scanning radiometers, their stability, the method of analyzing the data, and brief scientific results from the data.

2. Description of Instruments

The non-scanning package, shown in Fig. 1, consists of a pair of wide field-of-view (WFOV) radiometers, a pair of medium field-of-view (MFOV) radiometers, all of which were Earth-viewing, and a solar monitor. Each of these is an active cavity radiometer. Each pair of Earth-viewing channels has a total channel and a shortwave channel. The WFOV

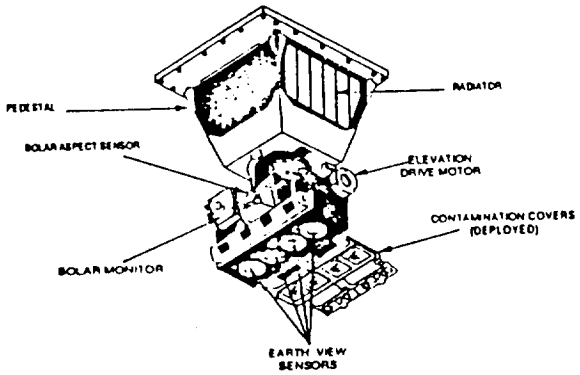

Figure 1. Non-scanning radiometer instrument.

channels view the Earth from one limb to the other. The MFOV channels each have an aperture which restricted its FOV to a circle with a 10° great circle diameter. Figure 2 shows the sensor design for the WFOV shortwave channel. In order to maintain the accuracy of their calibration while in orbit, the Earth-viewing channels are mounted on a beam which could rotate so that the instruments can look at internal blackbodies or through viewing ports at the Sun, as a high intensity well-known source, and at space for a near-zero radiance source. Thomas et al. (1992) have shown that the non-scanning radiometers have been quite stable, the shortwave channels having a gradual degradation which can be accounted for to a fraction of a percent by use of the on-board calibration system. Figure 3 shows the change with time in mean outgoing radiative flux at the top of the atmosphere (TOA) averaged over the portion of the Earth which is observed by the MFOV and WFOV non-scanning radiometers and the scanning radiometer. It is seen that with degradation accounted for by use of the on-board calibration systems, the change is on the order of 1 W/m^2.

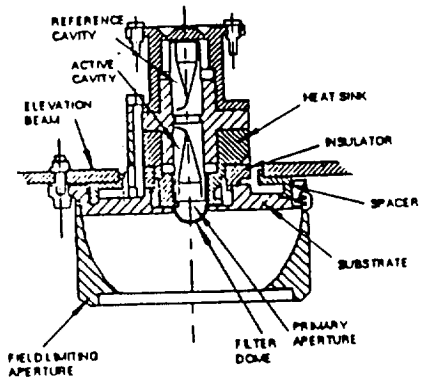

Figure 2. Wide field-of-View shortwave channel.

ERBE scanning and non-scanning radiometer packages were placed aboard three spacecraft. In October 1984, the Earth Radiation Budget Satellite was launched into an orbit with an inclination of 57°

and an altitude of 610 km, so that it precesses around the Equator every 72 days. The NOAA-9 operational spacecraft was placed into a near-polar (99° inclination) Sun-synchronous orbit with an altitude of 812

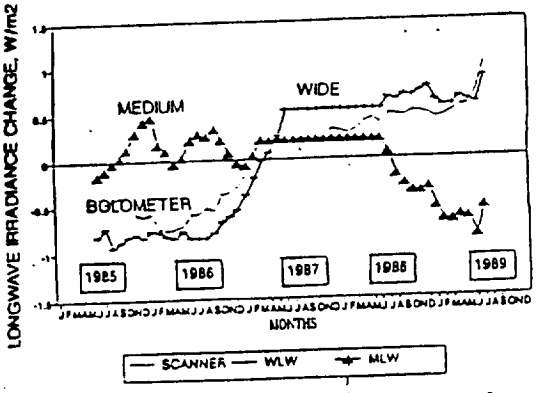

Figure 3. 12 months running mean at top of atmosphere for outgoing longwave radiation for ERBS.

km and an Equator crossing time of 1430 hours (ascending node). The NOAA-10 operational spacecraft was launched in October 1986 into a similar orbit (830-km altitude and 99o inclination) except for the Equator crossing time of 0730 hours. All three sets of non-scanning radiometers have operated continuously. At the time of this writing, all three spacecraft are operating well.

Figure 4 shows the availability of radiation measurements over the years. ERBE was proceeded by the Nimbus 6 and 7 ERB WFOV radiometers, which gave a low-resolution data record from 1975 through 1987 (Kyle et al., 1985), so that a 17-year record of low-resolution radiation data is available at present for studies, e.g., of interannual variations. The Clouds and Earth Radiant Energy System (CERES) aboard the Tropical Rainfall Measurement Mission (TRMM) is scheduled to begin providing scanning radiometer

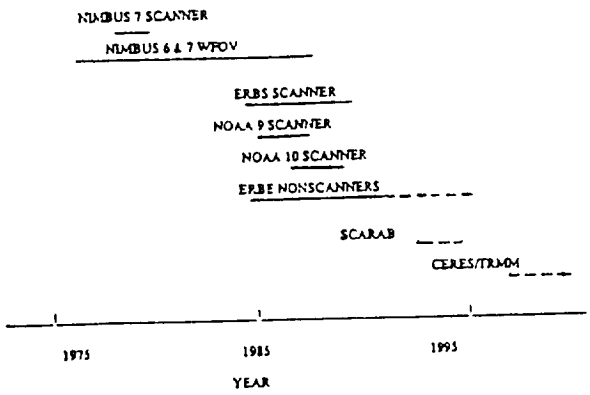

Figure 4. Time line of Earth radiation budget measurements.

data in 1997 over the Tropics, and the CERES aboard the first EOS platform should begin operation in 1998. In the meantime, the Franco-German-Russian SCAnning RAdiation Budget (SCARAB) radiometer (Kandel et al., 1992) is scheduled to fly aboard a Russian METEOR spacecraft in 1993 to fill the scanning-radiometer gap. However, most of the long-term radiation data record is from non-scanning radiometers.

3. Earth Viewing Data Analysis

The measurement equation for the non-scanning radiometers is

$$m(r_s) = \int_{FOV} L \cos\alpha \, d\Omega$$

where $m(r_s)$ is the measurement at the spacecraft position r_s, $L(r_s, v)$ is the radiance at the spacecraft from all directions within the FOV, α is the nadir angle of the incoming radiance, and $d\Omega$ is the differential solid angle. For the WFOV radiometers, the FOV is the entire Earth scene, from limb to limb. For the MFOV radiometers, the FOV is limited by an aperture to a circle with a 10° diameter great circle arc at the TOA. The longwave measurement is the total radiometer measurement minus the shortwave radiometer measurement. The radiance is related to the flux M(r) at TOA by the bidirectional reflectance function for shortwave and the limb-darkening function for longwave. These functions vary with the scene type and view angles and are denoted here as R(r,u), where u denotes the unit vector from r to r_s. The measurement equation can thus be written as

$$m(r_s) = \pi^{-1} \int_{FOV} M(r) R(r, u) \cos\alpha \, d\Omega$$

For the shortwave case, the TOA flux is given in terms of albedo $a(r)$, so that the measurement equation for the shortwave case becomes

$$m_S(r_s) = \pi^{-1} S \int_{FOV} a(r) R(r, u) \cos\varsigma \cos\alpha \, d\varsigma$$

where S is the solar output, i.e., the total solar irradiance normalized to mean Earth-Sun distance, ς is the

solar zenith angle at r, and the integration is over the sunlit FOV. The data analysis problem is to compute M(r) from $m(r_s)$ for the longwave case and $a(r)$ for the shortwave case. For ERBE, the Earth viewing non-scanning radiometer data have been analyzed using two methods: shape factor and numerical filter.

3.1 Shape Factor Method:

The shape factor method assumes that M(r) is constant over the FOV for the longwave case and that $a(r)$ is constant for the shortwave case. For the longwave case, the measurement equation simplifies to

$$m_L(r_s) = SF_L M(r_s)$$

$$= \pi^{-1} M(r_s) \int_{FOV} R(r, u) \cos\alpha d\Omega$$

and for the shortwave case the measurement equation becomes

$$m_S(r_s) = SF_S a(r_s)$$

$$= \pi^{-1} S a(r_s) \int_{FOV} R(r, u) \cos\varsigma \cos\alpha d\Omega$$

where SF_L and SF_S are the longwave and shortwave shape factors. For the WFOV, if $R(r, u)$ is independent of location, the longwave shape factor is the inverse of the square of the ratio of the orbit radius to the Earth's radius. During the period of time for which the scanning radiometers operated, scene identification data from the scanning radiometers (Wielicki and Green, 1989) were used to determine the appropriate $R(r, u)$ for computation of the shape factors. The longwave shape factor computed in this manner varied by only .25%, so the longwave shape factors were taken to be constants for data processing.

Studies were conducted by Green and Smith (1991) in which scenes of various types but constant over the FOV were assumed for the computation of the shortwave shape factors. Shape factors computed using the bidirectional reflectance function for mostly cloudy scene over ocean were found to produce shortwave fluxes at TOA that agreed with scanning radiometer results with a bias less than 1 W/m^2 and with standard deviations comparable to those obtained with the scene-dependent shape factor. This result is reasonable since the Earth's surface is three fourth ocean and since clouds do most of the reflecting on a global-wide basis. Non-scanning radiometer results have thus been processed in this manner after the cessation of the scanning radiometer on each spacecraft. The difference between the monthly mean shortwave maps (at $10^\circ \times 10^\circ$ resolution) using the mostly-cloudy-over-ocean scene identification rather than the full scene identification algorithm is less than 1 W/m^2 for most of the globe, with a few regions for which the difference is 1 to 2 W/m^2; there are three regions in which the difference is 4 W/m^2 for the medium FOV radiometers. The WFOV results are less sensitive. A study by Green (1983) showed that the resolution of a WFOV radiometer at an altitude of 820 km corresponds to a circle with a radius of 4o. Extensive validation studies were conducted for the scanning and non-scanning radiometers by Green et al. (1990).

3.2 Numerical Filter Method:

The numerical filter method is a one-dimensional resolution enhancement technique conceived by House and Jafolla (1980) as an improvement over the inherently low resolution of the shape factor approach. This approach treats the measurement equation as an integral equation to be solved for M(r) and $a(r)$. Because data are only available along the orbit track for periods of less than one orbit and no data are available in the cross track direction, the equations are considered to be one- dimensional and the solutions for M(r) and $a(r)$ are expressed as integrals over the orbit track. These integrals are discretized and stabilized, thereby producing the numerical filters, which are written in the form

$$M_j = \sum_{i=-N}^{N} \omega_i m_{j+i}$$

Here, M_j is the retrieved instantaneous flux at TOA, m_{i+j} are the measurements and the ω_i are filter weights. For ERBE, N = 6. "Measurements" are

taken to be 32-second averages of the radiometer output, which is sampled every 0.8 seconds. The effects of bidirectional reflectance function dependence on scene identification for these filters were studied as for the shape factor case, with similar results. The instantaneous TOA longwave fluxes and albedos from the shape factor and numerical filter analyses are archived for scientific investigations on magnetic tapes, denoted as S-7 data products.

4. Monthly Mean Maps

The TOA fluxes and albedo values obtained by each technique are compiled for each calender month, and the monthly mean outgoing longwave radiation and albedo are computed over the Earth, as described by Brooks et al. (1986), with modifications which were developed as a result of extensive validation investigations. The resulting monthly mean maps of absorbed solar radiation, based on these albedos, have been compared with scanning radiometer results by Rutan and Smith (1991). Rutan and Smith (1991) found that the accuracy of the monthly mean map could be improved by reconstructing the map with only the lowest 12 Fourier waves in longitude. This result is due to the sampling pattern in space and time for a non-scanning radiometer, which causes the major error source for a monthly map to be time variations rather than the lack of resolution. The sampling problem for a wide FOV radiometer has been studied by Salby (1988a and b). The radiation field for a day has a number of short-range transient features, whereas the monthly mean radiation field of the Earth is fairly smooth. Moreover, these transients move primarily in a west-east or east-west direction, so that longitudinal variations tend to be small (there are obvious exceptions in the major Equatorial convective regions and near coastlines). The RMS

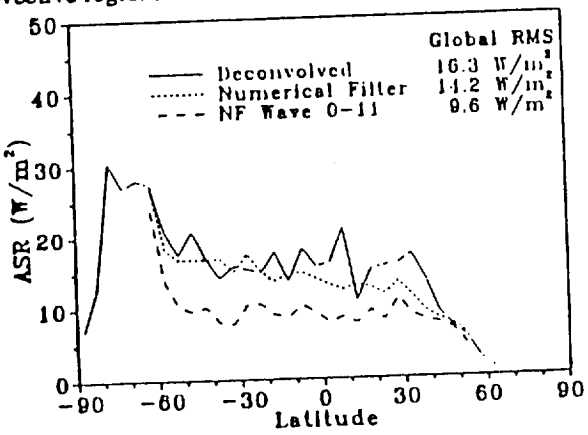

Figure 5. Zonal comparison of shortwave zonal averages.

accuracy of the non-scanner results vary with Sun-scene-satellite geometry for shortwave radiation, and its variation with latitude is shown in Fig. 5. Globally, with the Fourier filter eliminating longitudinal wavenumbers higher than 11, the RMS deviation of the numerical filter results from the scanning radiometer results at 5°x5° resolution was 9.6 W/m^2 and the RMS deviation of the zonal means was 3.5 W/m^2. The algorithm for the monthly mean maps has been modified and now places the derived fluxes not only in the 5°x5° grid-box containing the subsatellite point, but also in the adjacent grid-boxes in the crosstrack direction. These monthly maps are archived on magnetic tapes as S-10 data products.

5. Solar Output Measurements

The ERBE solar monitors have been shown to have an accuracy of 0.2%, with a precision better than 0.02% (Lee et al., 1991). Figure 6 shows the solar irradiance decreasing from 1984, when ERBE began producing data, until 1986, which was the minimum sunspot number and solar magnetic activity for sunspot cycle number 21. There was an increasing trend in solar irradiance from 1986 through 1989, when the maximum magnetic activity and sunspot numbers occurred for sunspot cycle number 22. The variation of solar irradiance over the measurement period is 0.1%.

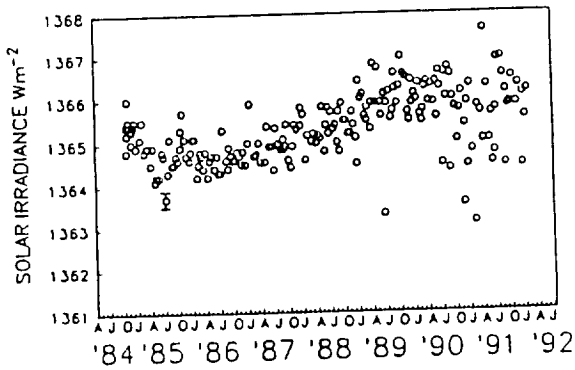

Figure 6. Solar irradiance based on ERBS solar monitor.

5. Conclusions

The ERBE non-scanning radiometers have provided a 7-year record of Earth radiation and solar output measurements thus far. The response of these radiometers are very stable. The monthly mean maps which are produced from the data have been shown to agree with the scanning radiometer results to 9.6 W/m^2 for 5°x5° resolution and to 3.5 W/m^2 for zonal

means. The time period of this record includes two ENSO events and a volcano to date. Measurements of solar output cover much of one solar cycle and agree very well with other measurements.

6. Data Availability

The scientific data products for the non-scanning radiometers, which are designated S-2, S-7 and S-10, are available from the National Space Science Data Center at the Goddard Space Flight Center of NASA, Greenbelt, Maryland, 20771.

References

Barkstrom, B. R. and G. L. Smith, 1986: The Earth Radiation Budget Experiment: Science and implementation, *Rev. of Geophys.*, **24**, 379-390.

Brooks, D. R., E. F. Harrison, P. Minnis, J. T. Suttles and R. S. Kandel, 1986: Development of algorithms for understanding the temporal and spatial variability of Earth radiation balance, *Rev. Geophys.*, **24**, 422-438.

Green, R. N., 1983: Accuracy and resolution of Earth radiation budget estimates, *J. Atmos. Sci.*, **40**, 977--985.

Green, R. N. and G. L. Smith, 1991: Shortwave shape factor inversion of Earth radiation budget observations, *J. Atmos. Sci.*, **48**, 390-402.

Green, R. N., F. B. House, P. W. Stackhouse, X. Wu, S. A. Ackermann, W. L. Smith and M. J. Johnson, 1990: Intercomparison of scanner and nonscanner measurements for the Earth Radiation Budget Experiment (ERBE), *J. Geophys. Res.*, **95**, 11,785-11,798.

House, F. B. and J. C. Jafolla, 1980: One-dimensional technique for enhancing Earth radiation budget observations from Nimbus 7 satellite, 1980 *International Radiation Symposium*, Fort Collins, Colorado.

Kandel, R. S., J. L. Monge, M. Viollier, L.A. Pakho mov, V. I. Adasko, R. G. Reitenbach and E. H. Raschke, 1992: The SCARAB Project: Earth Radiation Budget observations from the METEOR satellites, Presented at 29th COSPAR Plenary Meeting, Washington, D. C., U.S.A., August/September.

Kyle, H. L., P. E. Ardanuy and E. J. Hurley, 1985: The status of the Nimbus 7 Earth radiation budget data set, *Bull. Amer. Met. Soc.*, **66**, 1378-1388.

Lee, R. B., III, M. A. Gibson, S. Thomas, J. R. Mahan, J. L. Meckins and N. E. Tira, 1990: Earth Radiation Budget Experiment scanner radiometric calibration results. *Long-Term Monitoring of the Earth's Radiation Budget*, 1299, pp 80-91, Soc. Photo-optical Instrum. Eng., April 17 -18, Orlando, Florida.

Lee, R. B. III, M. A. Gibson, N. Shivakumar, R. Wilson, H. L. Kyle and A. T. Mecherikunnel, 1991: Solar irradiance measurements: Minimum through maximum solar activity, *Metrologia*, 265-268.

Luther, M. R., J. E. Cooper and G. R. Taylor, 1986: The Earth Radiation Budget Experiment nonscanning instrument, *Rev. of Geophys.*, **24**, 391-399.

Rutan, D. and G. L. Smith, 1991: Shortwave wide field-of-view results from the Earth Radiation Budget Experiment, *Proc. Seventh Symp. Met. Obs. & Instr.*, pp. 160-165, New Orleans, Louisiana, Jan. 13-15.

Salby, M., 1988a: Asynoptic sampling considerations for wide field-of-view radiometer measurements of outgoing longwave radiation. Part I: Spatial and temporal resolution, *J. Atmos. Sci.*, **45**, 1176-1183.

Salby, M., 1988b: Asynoptic sampling considerations for wide field-of-view radio meter measurements of outgoing longwave radiation. Part II: Diurnal and random space-time variability, *J. Atmos. Sci.*, **45**, 1184-1204.

Thomas, S., R. B. Lee, M. A. Gibson, R. S. Wilson and W. C. Bolden, 1992: In-flight shortwave calibration of the active cavity radiometers using tungsten lamps. *Instrumentation for Planetary and Terrestrial Atmospheric Remote Sensing*, **1745**, pp 227-234, Soc. Photo-optical Instrum. Eng., July 23-24, 1992, San Diego, California.

Wielicki, B. A. and R. N. Green, 1989: Scene identification for ERBE radiative flux retrieval, *J. Appl. Met.*, **28**, 1133-1146.